Small-angle neutron scattering from polymer solutions: 3. Semi-dilute solutions near the lower critical solution temperature

Randal W. Richards*
Department of Pure and Applied Chemistry, University of Strathclyde, Glasgow G1 1XL, UK
and Ann Maconnachie and Geoffrey Allen
Department of Chemical Engineering and Chemical Technology, Imperial College, London SW7 2BY, UK
(*Received* 4 *June* 1980; *revised* 4 *August* 1980)

Measurements of the radius of gyration and the screening lengths have been made for semi-dilute solutions of polystyrene near the lower critical solution temperature. From these data two regions of behaviour are clearly discerned. By analogy with similar data near the upper critical solution temperature, a 'phase diagram' has been drawn from the results around the lower critical solution temperature.

INTRODUCTION

A phenomenological description of concentrated polymer solutions has been provided in Part 2 of this series[1]. Results presented there and in Part 1[2] indicated that other regions of behaviour are present apart from those predicted by scaling laws[3]. Notwithstanding this, the scaling law approach and the subsequent phase diagram obtained have provided an excellent description of polymer solutions, especially in the semi-dilute concentration range[2,4]. Evidence for this region and its behaviour in accordance with scaling laws has been obtained not only from small-angle neutron scattering (SANS) studies but also from sedimentation velocity and photon correlation spectroscopy measurements[2,4-10].

To our knowledge investigations thus far published have been in the region of the upper critical solution temperature, the Flory or theta (θ) temperature. We report here the results of SANS experiments on semi-dilute solutions of polystyrene over a temperature range covering the lower critical solution temperature (sometimes termed the Rowlinson temperature).

THEORY

The construction of a 'phase' diagram of polymer solution behaviour is based on the identification of the Flory theta temperature as a tricritical point in the sense of magnetic phase transitions[11]. Polymer solutions display 'ideal' behaviour at a second, higher temperature, the lower critical solution temperature (*LCST*)[12]. Intuitively then, we would expect that there should be different behaviour regimes in the neighbourhood of this lower critical solution temperature. Hence, the full phase diagram encompassing both temperature regions should be as shown in *Figure 1*.

Whilst there is a large amount of theoretical work on the thermodynamics of polymer solutions at or near the *LCST*[13,14], results concerning dimensions of polymers are somewhat scanty and totally concerned with dilute solutions. However, the evidence that is available (cloud point curves[15], viscometry[16,17], and light scattering[18]) supports the notion of ideal behaviour prevailing at the *LCST*. The phenomenon of an *LCST* in polymer solutions is intimately associated with the expansion properties of the solvent (in the absence of specific interactions such as hydrogen bonding). Since the *LCST* is generally close to the gas–liquid critical temperature of the solvent, the solvent can no longer be treated as an incompressible fluid. Theoretical descriptions of polymer dimensions in this region must therefore take this into account[19]. Whilst this may be done implicitly by using corresponding states expressions for χ_1 [12,13], the polymer–solvent interaction parameter, no rigorous explicit theory has yet been derived to our knowledge.

To describe the lines C_L^* and C_L^{**} dividing the behaviour regions near the *LCST* we have empirically adapted the existing formulae for these lines near the *UCST*[15]. This approach is used in the absence of a rigorous theory of polymer dimensions near the *LCST*. The line C^* separates the dilute good solution regime from the semi-dilute region where molecules overlap and is described by the relation:

$$C^* \approx N^{-4/5}\tau^{-3/5} \tag{1}$$

The line C^{**} separates the semi-dilute region from the concentrated solution region where polymers have their bulk dimensions and is given by:

$$C^{**} \sim \tau \tag{2}$$

Finally, in this section there is a line which separates the

* To whom correspondence should be addressed.

0032-3861/81/020153-05$02.00
© 1981 IPC Business Press

dilute solution region from the dilute theta region (I') where molecules have unperturbed dimensions. This is defined by:

$$\tau\sqrt{N}=1 \tag{3}$$

In all the above relationships N is the number of monomer units in the chain and τ is a reduced temperature. Near the $UCST$ the reduced temperature is written as:

$$\tau=(T-\theta)/\theta \tag{4}$$

This relationship has theoretical justification since it arises in the renormalization group theory of magnetic spin sytems[3]. Furthermore, the temperature dependence of polymer chain dimensions are frequently linear in $(T-\theta)$ near the $UCST$[20].

The form of equation (4) raises difficulties near the $LCST$, where θ now becomes θ_L, since for the temperature range over which measurements are made $T \leqslant \theta_L$. Consequently, equation (1) becomes indeterminate. This problem can be overcome if we use

$$-\{|[(T-\theta_L)/\theta_L]|^{3/5}\}$$

By this means we can retain all the expected behaviour: i.e. a positive ordinate for $T>\theta_L$ and a decrease in C^* for temperatures less than θ_L due to chain expansion.

EXPERIMENTAL

Both materials used and the techniques of small-angle neutron scattering for determination of the mean square radius of gyration ($\langle s^2\rangle_w$) and the screening length (ξ) were with one exception, exactly as described in Part 2 of this series[1].

The exception was in the cells used to contain the solutions. Over the temperature range utilized, $60 \leqslant T(^\circ C) \leqslant 210$, cyclohexane develops a considerable vapour pressure ~ 20 atm at 200°C. Consequently the solutions were enclosed in silica tubing of 2 mm internal diameter and 4 mm external diameter. The solutions were outgassed by repeated freeze–thaw cycles under high vacuum, they were then flame-sealed under vacuum. Using cells of this type, no breakages were encountered during the performance of the experiments.

Solutions

The influence of temperature on the radius of gyration of polystyrene in cyclohexane was investigated for one semi-dilute solution. A total polymer concentration of 0.179 g ml^{-1} was used, the concentration of deuteropolystyrene being 0.02 g ml^{-1}.

Screening lengths as a function of temperature were measured for three solutions of hydrogenous polystyrene in deuterated cyclohexane. The concentrations were: 0.099 g ml^{-1}; 0.183 g ml^{-1}; and 0.274 g ml^{-1}. All concentrations are quoted for a temperature of 25°C.

RESULTS

Radius of gyration

The intensity of neutrons scattered from solutions containing deuterated polystyrene (PSD) were corrected for incoherent background scattering by subtracting the scattered neutron intensity of a solution of hydrogenous polystyrene (PSH) in cyclohexane. The excess of scattered intensity was plotted according to equation (1) in Part 2[1] of this series and the mean square radii of gyration corrected to weight-average values in the same manner. *Figure 2* shows the dependence of $\langle s^2\rangle_w$ on temperature.

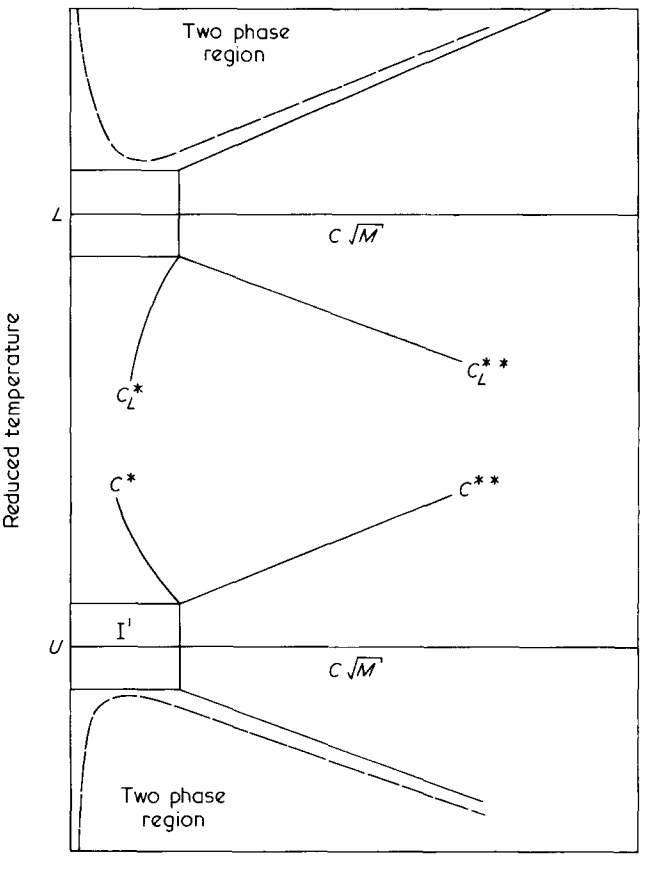

Figure 1 Schematic temperature–concentration diagram for polymer solutions incorporating the proposed extension to the lower critical solution temperature. L = Position of lower critical solution temperature; U = position of upper critical solution temperature

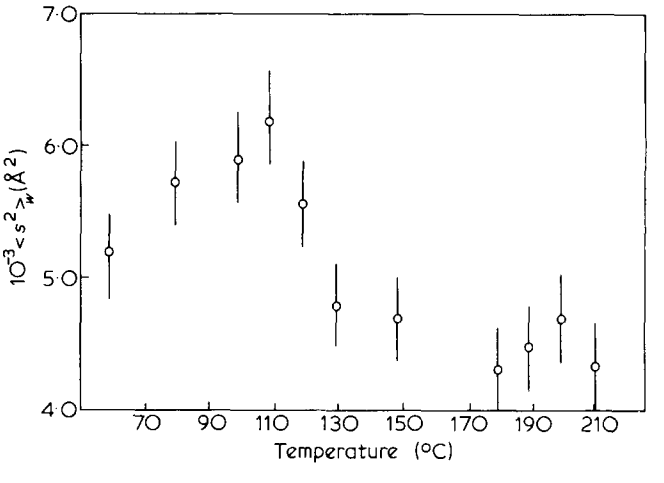

Figure 2 Mean square radius of gyration of deuteropolystyrene in cyclohexane ($C_{polymer}$ = 0.179 g ml^{-1}) as a function of temperature

Screening lengths

Typical plots of $I(Q)^{-1}$ as a function of Q^2 at three different temperatures are shown in *Figure 3* for the 18%

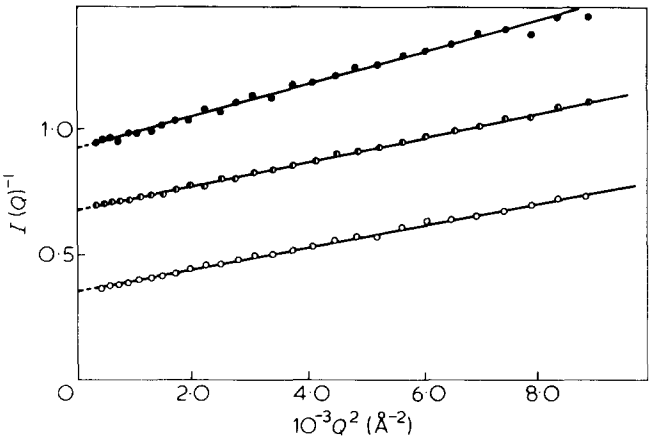

Figure 3 Reciprocal scattered neutron intensity $[I(Q)^{-1}]$ as a function of squared scattering vector (Q^2) for a solution of hydrogenous polystyrene in deuterocyclohexane at three different temperatures: ○, 60°C; ◐, 131.6°C; ●, 201.9°C

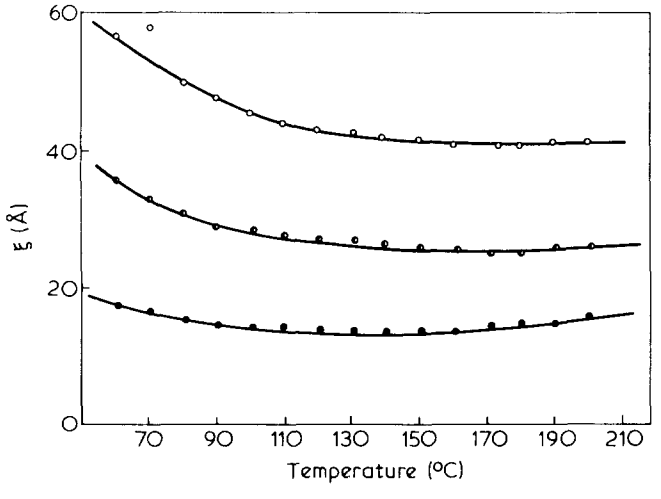

Figure 4 Variation of screening length (ξ) with temperature for polystyrene in cyclohexane. ○, C = 0.099 g ml^{-1}; ◐, C = 0.183 g ml^{-1}; ●, C = 0.274 g ml^{-1}

solution of PSH in deuterocyclohexane. Similar plots for other concentrations examined (27.4 and 9.9%) had an identical shape to that shown in *Figure 3*. Screening lengths, ξ, were calculated from the slope and intercepts of the plots in accordance with equation (2) of Part 2[1] of this series. *Figure 4* shows the variation of screening length for each of the solutions over the temperature range investigated.

None of the plots of $I(Q)^{-1}$ as a function of Q^2 showed any evidence of a 'crossover' in the scattering law remarked on in Part 2.

DISCUSSION

Referring to *Figure 2* there appear to be three distinct regions in the dependence of $\langle s^2\rangle_w$ on temperature. Between 60° and ~100°C there is an increase in $\langle s^2\rangle_w$ with temperature which we interpret as a continuation of the behaviour observed between ~40° to 65°C in Part 1[2] of this series. According to renormalization group theory[3,4], the dimensions of polymer molecules in semi-dilute solution should have no temperature dependence in a finite region near the *UCST* (Region I′ in *Figure 1*). At somewhat higher temperatures the dimensions should become temperature dependent and obey the relation below:

$$\langle s^2\rangle_w \propto (T-\theta)^{0.25}$$

(see Part 2, *Table 1*). A log–log plot of our earlier data[2] is shown in *Figure 5* and includes the present data between 60° and 100°C. A line of slope 0.25 has been drawn through the temperature-dependent points and fits tolerably well with the data.

As the temperature approaches the *LCST*, then, according to our extension of the theory, the chain dimensions should decrease with increasing temperature, eventually becoming constant at the unperturbed value over a finite temperature range near the *LCST*.

From *Table 1* in Part 2, the dependence of $\langle s^2\rangle_w$ is:

$$\langle s^2\rangle_w \approx N\rho^{-1.4}\beta^{1.4}$$

from scaling laws near the *UCST*, and:

$$\beta \propto (T-\theta)/\theta = \tau$$

As we have remarked earlier, τ becomes negative when $\theta = \theta_L$, consequently in plotting the data to discern the presence of different behaviour regimes we have used $|(T-\theta_L)|$. A plot of $\log\langle s^2\rangle_w$ as a function of $\log|(T-\theta_L)|$ is shown in *Figure 6*. We have used a value of 213°C for the θ_L of polystyrene in cyclohexane derived from phase separation work of Saeki *et al.*[15].

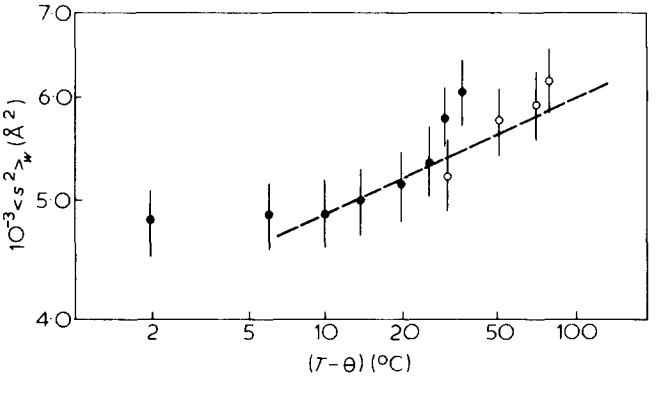

Figure 5 Log–log plot of $\langle s^2\rangle_w$ as a function of $(T-\theta)$ for polystyrene in cyclohexane C = 0.179 g ml^{-1}, θ = 30°C. ●, Earlier data; ○, present data

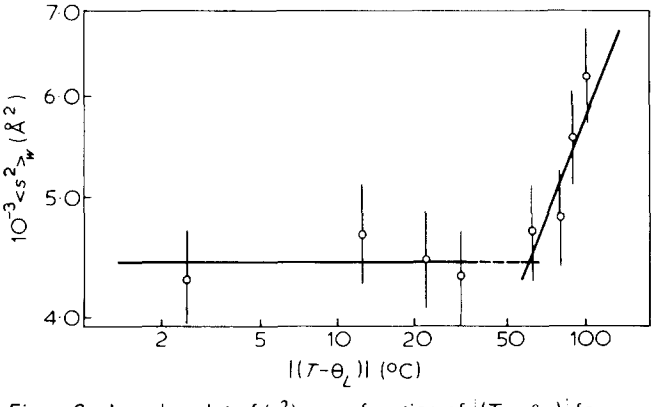

Figure 6 Log–log plot of $\langle s^2\rangle_w$ as a function of $|(T-\theta_L)|$ for polystyrene in cyclohexane θ_L = 213°C

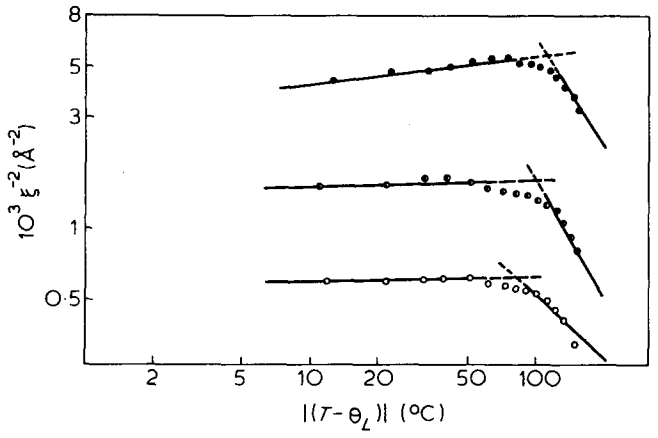

Figure 7 Log–log plot of ξ^{-2} as a function of $|(T-\theta_L)|$ for three different concentrations of polystyrene in cyclohexane. Symbols as in *Figure 4*

The lines drawn through the data points are empirical best fits. The slope of the temperature dependent line is approximately 0.52, which is twice that predicted in the neighbourhood of the *UCST* by either scaling law[3,4] or mean field theories[21]. Notwithstanding this, it is evident that two regions of behaviour exist in the region of the *LCST*. From *Figure 6* the temperature at which this crossover in behaviour takes place for this solution (concentration = 0.179 g ml^{-1} at 25°C) is $|(T-\theta_L)| = 63° \pm 5$°C.

Turning now to the screening length, similar behaviour should be apparent as the temperature increases. That is, the screening length should be temperature dependent until the crossover line C_L^{**} is reached. At this point, the screening length is no longer temperature dependent but only concentration dependent[3]. Consequently, the crossover temperature should be concentration dependent. These features are discernible in *Figure 4*, but the crossover temperatures are much more distinct in *Figure 7*, where we have plotted $\log \xi^{-2}$ as a function of $\log|(T-\theta_L)|$, a form which is suggested by the formulae for ξ[2,4]. The two regions of behaviour are now clearly evident. Best straight lines have been drawn through the data. The crossover values have been determined from the intersection of the two straight lines in each case. The following results were obtained:

$$C = 0.099 \text{ g ml}^{-1};\ |(\theta_L - T)| = 83°\text{C}$$

$$C = 0.183 \text{ g ml}^{-1};\ |(\theta_L - T)| = 102°\text{C}$$

$$C = 0.274 \text{ g ml}^{-1};\ |(\theta_L - T)| = 115°\text{C}$$

Whilst two regions of behaviour are evident in *Figure 7*, there appears to be no region of temperature where ξ^{-2} does not change with temperature. We attribute the weak temperature-dependent regions in *Figure 7*, i.e. the lines with positive slope, to the changing concentration of the solutions. At the temperatures in question, ~120° to 200°C, the solvent is expanding rapidly, thus effectively decreasing the polymer concentration in the solution. Since $\xi^{-2} \propto C^{3/2}$, then as C decreases so will ξ^{-2}.

Construction of the temperature–concentration diagram near the LCST

The procedure used by Cotton *et al.*[4] for the *UCST* case is followed here. In accordance with them we use axes of $(T-\theta_L)\sqrt{M}$(°C) and $C\sqrt{M}$ (g ml^{-1}) which removes any dependence on molecular weight but presumes a specific $(T-\theta)$-type dependence for the excluded volume.

The basis of this diagram is the line C_L^{**} shown in *Figure 1*, which in our case is $C_L^{**}\sqrt{M}$. This line is described by equation (2), which, for the axes used here, becomes:

$$C_L^{**}\sqrt{M} \sim (T-\theta_L)\sqrt{M}$$

This line must pass through the origin and the four crossover temperatures determined from the variation of radius of gyration and screening length discussed above. Concentrations, C^{**} at the crossover temperature, have been obtained from the values at 25°C and corrected using the known density and temperature coefficient of density for cyclohexane[22]. These points and the line constructed from them are shown in *Figure 8*. The vertical line corresponds to $C_\theta^*\sqrt{M}$, where C_θ^* is the concentration at which molecules with unperturbed dimensions begin to overlap. This concentration is defined by the inequality:

$$\frac{3M}{4\pi N_A \langle s^2\rangle_w \theta^{3/2}} \leqslant C_\theta^* \leqslant \frac{M}{N_A \langle s^2\rangle_\theta^{3/2}}$$

We have used the lower bound to calculate $C_\theta^*\sqrt{M}$, since other evidence[23] appears to show that overlap begins at lower concentrations than suggested by viewing the polymer molecule as a hard sphere and certainly much lower than the cube shape implicit in $C_\theta^* = M/N_A\langle s^2\rangle_\theta^{3/2}$. The full horizontal line drawn from the intersection of this vertical with $C^{**}\sqrt{M}$ line separates the theta region from the dilute good solvent regime.

The intersection of these three lines is used to calculate the $C^*\sqrt{M}$ line which separates the dilute good solvent region from the semi-dilute region. The equation we have used for this line is:

$$C^*\sqrt{M} = -\sqrt{M}|(T-\theta_L)|^{-3/5}$$

Additional experimental evidence for the existence of a temperature–concentration diagram in the region of the

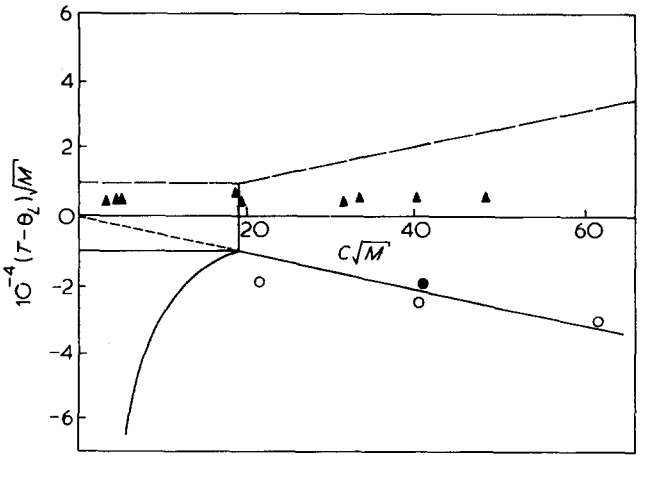

Figure 8 Temperature–concentration diagram for polystyrene in cyclohexane near the lower critical solution temperature. ○, Data points from screening length measurements; ●, data point from radius of gyration measurements; – – – –, theoretical asymptotes of phase separation curve; ▲, phase separation data obtained by Saeki *et al.*[15]

LCST is not available. A technique which could be used to show the existence of the $C^*\sqrt{M}$ line is the use of photon correlation spectroscopy to measure the translational diffusion coefficient. Quite definite breaks have been observed in log–log plots of the diffusion coefficient as a function of concentration near the *UCST*[23]. However, the practical difficulties in using a temperature range up to 200°C may prevent such experiments.

Phase separation data at the *LCST* should provide some support for the existence of such regions. If the full scaling law analysis can be applied near the *LCST*, then there is a line symmetric to the $C^{**}\sqrt{M}$ line about $(T-\theta_L)\sqrt{M}=0$. This symmetric line, and others, are drawn as broken curves in *Figure 8*. This line should be the asymptote of one branch of the phase separation curves plotted as $(T-\theta_L)\sqrt{M}$ against $C\sqrt{M}$. The symmetric horizontal line should be at the maximum of this composite phase separation curve.

Figure 8 shows data points abstracted from published phase separation curves for polystyrene in cyclohexane[15]. Unfortunately, the data does not cover a wide enough range in polystyrene concentration, and all the points fall on a horizontal line which is somewhat displaced from the theoretical value.

CONCLUSION

From the results presented it is evident that there are at least two regions of distinct behaviour in the region of the *LCST*. A 'phase' diagram can be constructed but supporting evidence is scarce. It appears then that the lower critical solution temperature may also be treated as a tricritical point as defined by de Gennes.

The results have demonstrated the ability of SANS to obtain data which is either unobtainable or only obtained with difficulty by other techniques.

ACKNOWLEDGEMENTS

We thank our ILL local contacts Dr R. Duplessix and Dr P. Timmins for their assistance. One of us (R.W.R.) thanks AERE, Harwell, for an EMR grant during the time these measurements were made.

REFERENCES

1 Richards, R. W., Maconnachie, A. and Allen, G. *Polymer* 1980, **21**, 000
2 Richards, R. W., Maconnachie, A. and Allen, G. *Polymer* 1978, **19**, 266
3 Daoud, M. and Jannink, G. *J. de Physique* 1975, **37**, 973
4 Cotton, J. P., Nierlich, M., Boué, F., Daoud, M., Farnoux, B., Jannink, G., Duplessix, R. and Picot, C. *J. Chem. Phys.* 1976, **65**, 1101
5 Daoud, M., Cotton, J. P., Farnoux, B., Jannink, G., Sarma, G., Benoit, H., Duplessix, R., Picot, C. and de Gennes, P. G. *Macromolecules* 1975, **8**, 804
6 Nierlich, M., Cotton, J. P. and Farnoux, B. *J. Chem. Phys.* 1978, **69**, 1379
7 Pouyet, G., Francois, J., Dayantis, J. and Weill, G. *Macromolecules* 1980, **13**, 176
8 Roots, J. and Nystrom, B. *Polymer* 1979, **20**, 148
9 Adam, M., Delsanti, M. and Jannink, G. *J. de Physique Lett.* 1976, **37**, L53
10 Allen, G., Vasudevan, P., Hawkins, E. Yvonne, and King, T. A. *J. Chem. Soc. (Faraday Trans. II)* 1977, **73**, 449
11 de Gennes, P. G. *J. de Physique Lett.* 1975, **46**, L55
12 Patterson, D., Delmas, G. and Somcynsky, T. *Polymer* 1967, **8**, 503
13 Patterson, D. *Pure Appl. Chem.* 1972, **31**, 133
14 Höcker, H., Shih, H. and Flory, P. J. *Trans. Faraday Soc.* 1971, **67**, 2275
15 Saeki, S., Kuwahara, N., Konno, S. and Kanenko, M. *Macromolecules* 1973, **6**, 246
16 Kuwahara, N., Saeki, S., Konno, S. and Kanenko, M. *Polymer* 1974, **15**, 66
17 Richards, R. W., *Polymer* 1980, **21**, 715
18 Delmas, G. and Patterson, D. *Polymer* 1966, **7**, 513
19 Sanchez, I. C. *Macromolecules* 1979, **12**, 980
20 Berry, G. C. *J. Chem. Phys.* 1966, **44**, 4550
21 Edwards, S. F. and Jeffers, E. F. *J. Chem. Soc. (Faraday Trans II)* 1979, **75**, 1020
22 Johnson, B. L. and Smith, J. Ch. 2 in 'Light Scattering from Dilute Polymer Solutions'. (Ed. M. B. Huglin) Academic Press, London, 1972
23 Hadgraft, J., Hyde, A. J. and Richards, R. W. *J. Chem. Soc. (Faraday Trans II)* 1979, **75**, 1495